microplastics

MDPI

Article

Evaluating the Environmental Factors on Microplastic Generation: An Accelerated Weathering Study

Sara Rostampour [1,2], Song Syun Jhang [1,3], Jung-Kai Hsu [1,3], Rachel Cook [1,4], Yuejin Li [2], Chunlei Fan [2] and Li-Piin Sung [1,*]

[1] Engineering Laboratory, National Institute of Standards and Technology, Gaithersburg, MD 20899, USA; saros4@morgan.edu (S.R.); zx55kk55aa@gmail.com (S.S.J.); jungkai.hsu@nist.gov (J.-K.H.); rachel.cook@ua.edu (R.C.)
[2] Bio Environmental Science Program, Morgan State University, Baltimore, MD 21251, USA; yuejin.li@morgan.edu (Y.L.); chunlei.fan@morgan.edu (C.F.)
[3] Department of Materials Science and Engineering, National Cheng Kung University, Tainan 70101, Taiwan
[4] Department of Metallurgical and Materials Engineering, University of Alabama, Tuscaloosa, AL 35487, USA
* Correspondence: li-piin.sung@nist.gov

Abstract: Microplastics pose a significant environmental threat, and understanding their sources and generation mechanisms is crucial for mitigation efforts. This study investigates the effects of ultraviolet intensity, temperature, and relative humidity on the degradation of polyethylene terephthalate (PET) plastics and the subsequent formation of microplastic particles. PET samples were exposed to ultraviolet (UV) radiation under various environmental conditions using the SPHERE (Simulated Photodegradation via High Energy Radiant Exposure) accelerated weathering device at the National Institute of Standards and Technology (NIST). Attenuated total reflectance–Fourier transform infrared spectroscopy (ATR-FTIR) and laser confocal scanning microscopy (LSCM)/atomic force microscopy (AFM) were employed to characterize the chemical and morphological changes on the weathered surfaces. This study's findings reveal that temperature and relative humidity significantly influence the rate of photodegradation and the characteristics of the generated microplastics. Higher temperatures and increased humidity accelerated the degradation process, leading to a higher abundance of microplastic particles. However, larger particles were observed at higher temperatures due to aggregation. These results underscore the importance of considering environmental factors when assessing the fate and transport of microplastics in the environment. Developing strategies to reduce plastic pollution and mitigate the generation of microplastics is essential for protecting ecosystems and human health.

Keywords: accelerated weathering; atom force microscopy; confocal laser scanning microscopy (LSCM); photodegradation; microplastics (MPs); morphological change; polyethylene terephthalate (PET); surface roughness; UV radiation

Academic Editor: Nicolas Kalogerakis

Received: 13 January 2025
Revised: 20 February 2025
Accepted: 26 February 2025
Published: 5 March 2025

Citation: Rostampour, S.; Jhang, S.S.; Hsu, J.-K.; Cook, R.; Li, Y.; Fan, C.; Sung, L.-P. Evaluating the Environmental Factors on Microplastic Generation: An Accelerated Weathering Study. *Microplastics* **2025**, *4*, 13. https://doi.org/10.3390/microplastics4010013

1. Introduction

Plastic has become a ubiquitous material in contemporary society, permeating nearly every aspect of our daily lives, and it is estimated to reach a total of 33 billion tons by 2050 [1]. Over the past few decades, polyethylene terephthalate (PET) has been widely used in various plastic products [2]. PET is a thermoplastic polymer widely employed in food packaging applications, particularly bottles, and engineering plastics. Its popularity is attributed to its cost-effectiveness, low weight, resistance to carbon dioxide permeation,

and optical transparency [3–5]. Each year, an estimated 300 million tons of plastic waste are generated worldwide, with around 12.7 million tons reaching the oceans. Plastic waste can linger and accumulate as hazardous environmental contamination for centuries [6,7]. Photodegradation rate depends on factors like polymer type, shape, and intended use. Environmental factors such as exposure to sunlight, humidity, and temperature can accelerate the breakdown of plastics, leading to the formation of microplastics [8,9].

Microplastics found in water bodies can be categorized into two main groups: primary microplastics and secondary microplastics [8]. The size of both primary and secondary microplastics ranges from 1 µm to 5 mm. Primary microplastics (from consumer products like cosmetics, personal care items, cleaning agents, and paints) are a major source of marine pollution when released into sewage effluent [10]. Secondary microplastics are produced through the weathering and degradation of larger plastic pieces, leading to adverse effects on ecosystems and human health [11–13]. The accumulation of non-degradable microplastics has been identified as a toxic threat to aquatic life [14–16]. The accidental consumption of microplastics by animals can pose serious health risks, and plants growing in microplastic-contaminated soil may also suffer physiological consequences [17]. Also, microplastics in agricultural soils originate from various sources, including air deposition, agricultural practices, and irrigation, and can potentially affect agricultural products [18]. Secondary microplastics have been detected in the digestive systems of various aquatic organisms, ranging from benthic invertebrates to larger mammals. As these microplastics are transferred through the food web, and growing concerns about their detrimental effects on marine life have emerged [19,20]. Both direct and indirect evidence supports the adverse impacts of microplastics, including interference with reproduction, increased mortality, and a dose-dependent relationship with physiological stress. These effects manifest in behavioral changes, immune system disruptions, metabolic abnormalities, and altered energy balance [1,21–23]. Moreover, recently discovered microplastics in commonly used sea salts raise concerns about potential health implications for human consumption [8]. Microplastics, with their potential to harm both human health and the environment, represent a particularly severe form of plastic pollution [24].

The morphology of the plastic surface changes and evolves as it is exposed to environmental factors. While standard plastics have a smooth flat surface, weathered plastics often exhibit a rough and uneven texture, characterized by cracks, fractures, pits, and numerous small fragments. A study conducted on Hawaii's beaches revealed that polyethylene (PE) exposed in the natural environment exhibits a higher frequency of pits and fractures compared to polypropylene (PP), suggesting that PE is more prone to oxidation [25]. An accelerated exposure study found that the surface appearance of low-density polyethylene (LDPE) underwent significant changes after 375 h and 500 h of exposure, characterized by the formation of surface cracks and increased roughness [26]. Scanning electron microscope (SEM) images of the LDPE bar surface revealed the development of microcracks during the initial 800 h of exposure. A more pronounced crack pattern became evident after a prolonged UV exposure of 3200 h [27]. Surface pits and erosion began to appear in polyvinyl chloride (PVC) after approximately 400 h of UV exposure, with their frequency and size increasing noticeably over time [28].

PET, a thermoplastic semicrystalline material, undergoes degradation that affects both its chemical and physical properties, including chain conformation, crosslinking, branching, crystallinity, and color [29]. While fresh PET surfaces are typically smooth and transparent, degraded PET often exhibits roughness, brittleness, yellowing, and irregular cracks and pits. These physical changes, including cracking, embrittlement, yellowing, and flaking, are common signs of PET degradation PET [30,31]. An accelerated study found that exposure to UV light and water led to significant surface damage on the PET samples, including cracking and surface

ruptures [32]. The photo-oxidation of PET involves the oxidation of CH_2 groups near the ester linkages, forming hydroperoxide species. These species can then decompose to produce photodegradation products like carboxylic acids through different chemical reactions [33].

Several investigations have explored how factors such as temperature, humidity, and the intensity of UV exposure influence PET's degradation rates and mechanisms [34–37]. While PET can degrade through thermal oxidation, hydrolytic cleavage and photo-oxidation induced by UV light are more prevalent in typical environmental conditions [34]. The photolytic cleavage of the ester bond in PET triggers degradation, releasing carbon monoxide (CO), carbon dioxide (CO_2), terephthalic acid, anhydrides, carboxylic acids, and esters [38]. The environmental aging of PET results in both chemical changes and morphological alterations, characterized by the emergence of a microcrack network in the surface layer of the degraded polymer, ultimately leading to plastic fracture [39]. At high UV irradiance, PET exhibits a non-linear relationship between irradiation and yellowing, with increased irradiation leading to more intense yellowing. This diffusion-limited oxidation allows for the accumulation of yellow products primarily generated through photochemical reactions [40]. A study found that degradation was most significant at 100% relative humidity, followed by moist soil (45% RH) and dry soil at 70 °C. However, this trend was reversed at higher temperatures (80 °C and 90 °C), where degradation rates were faster in wet soil compared to 100% relative humidity [6].

The impact of UV radiation on weathering processes can be intricate, often interacting with other elements like temperature and humidity. Many prior studies on the photodegradation of PET have focused on investigating chemical changes in PET properties. This leaves gaps in our knowledge of how these environmental factors collectively influence the molecular structure and physical appearance of PET. To fully understand microplastic formation, new questions about how polymer degradation and fracturing processes are influenced by environmental aging need to be explored. The chemical, previously shown to destabilize the amorphous regions of the polymer in our earlier work [34], induced morphological changes on the PET surface. This study aims to systematically examine the effects of UV exposure duration, humidity, and temperature on the morphological structure of PET under simulated environmental conditions. Laser scanning confocal microscopy (LSCM) and atomic force microscopy (AFM) were employed to identify morphological changes in the PET surface during UV irradiation. This study's findings reveal how PET degrades in different environments, leading to the formation of microplastics. By understanding the factors that contribute to microplastic formation, strategies can be developed to reduce plastic pollution and protect ecosystems.

2. Materials and Methods

2.1. Sample Preparation and Weathering

Materials used for this study were PET films obtained from the top portion of post-consumer water bottles. The film dimension (rectangular pieces) was approximately (3 to 4) cm by (2 to 3) cm. PET samples were placed in a PIE (Photochemical Internal Environment) sample holder within the SPHERE (Simulated Photodegradation via High Energy Radiant Exposure) weathering device at the National Institute of Standards and Technology (NIST)) chambers. The PIE sample holder (as shown in Figure 1) has four individually sealed compartments that can accommodate individual PET film exposed to a fixed humidity level or in a liquid environment. The saturated humidity condition was achieved by injecting 0.2 mL of distilled water using a syringe to maintain saturated humid air at 50 °C throughout the exposure period. The relative humidity (RH) level was measured using a temperature/humidity sensor in the enclosure of the PIE sample compartment. The daily UV dose was around 13.8 MJ/m^2 from 295 nm to 400 nm. Exposure

conditions included three different temperatures (30 °C, 40 °C, and 50 °C) and two different levels of humidity: dry (<5% RH) and saturated humidity (>95% RH, labeled as *SH* later in the text). PET samples were exposed to UV radiation for up to 20 days, equivalent to approximately one year of natural UV irradiation (annual UV dose is around 294 MJ/m^2) in Florida [41,42],and were retrieved every two days for characterization. There were at least three replicates in each exposure condition. Attenuated total reflectance–Fourier transform infrared spectroscopy (ATR-FTIR) and laser confocal scanning microscopy (LSCM)/atomic force microscopy (AFM) were used for measuring the chemical and morphological changes on the weathered surfaces, respectively.

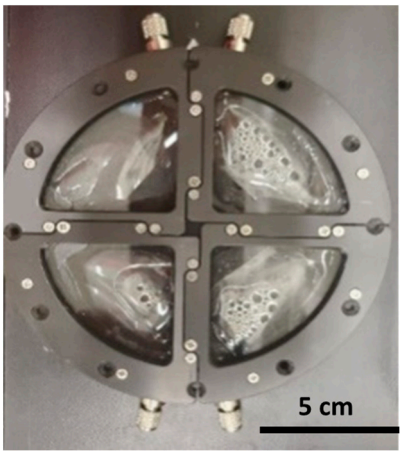

Figure 1. Photo of PIE sample holder with four individually sealed compartments.

2.2. Characterizations

This paper focuses on surface morphological changes and microplastic particle formation. The surface morphology and surface roughness were characterized mainly by laser scanning confocal microscopy (LSCM), while, for the high-resolution imaging of micro-/nano-plastic particles (height and shape), atomic force microscopy (AFM) was used.

2.2.1. Laser Scanning Confocal Microscopy (LSCM)

A reflectance LSM 800 laser scanning confocal microscope (Carl Zeiss Microscopy LLC, Thornwood, NY, USA) was used. Images were taken with laser wavelength at 561 nm and 50×/0.5, 150×/0.95 air lens at scanning z-step of 0.1 µm. The LSCM images presented in this paper were in two-dimensional (2D) projection (an image formed by summing the stack of images over the z-direction). Each frame consisted of 1024 pixels × 1024 pixels, or 255.56 µm × 255.56 µm, in size. The root-mean-square (RMS) surface roughness (S_q) values were calculated using Zeiss ConfoMap ST software (version 7.4.8341) using ISO 25178 standard analysis [43] within a scanning area of 255.56 µm × 255.56 µm. Five locations per sample were randomly selected for imaging and topography data collection. A freeware ImageJ (version 1.46r, Wayne Rasband, NIH, Bethesda, MD, USA) was used to characterize the quantity and size of the particles formed on the degraded surface of the PET. Five images per sample and repeated analysis were conducted to ensure accurate and reliable results. Measurement uncertainties were calculated using standard deviations (SDs) from at least 15 images (n = 15).

2.2.2. Atomic Force Microscopy (AFM)

A Bruker Dimension Icon AFM microscope (Bruker, Billerica, MA, USA) was used in the tapping mode. The phase differences reflect the tip–sample interaction and the properties of individual components in heterogeneous materials. In this study, both height and phase images were recorded simultaneously with a (512 × 512) pixel resolution at a scan rate of

0.3 Hz by an antimony-doped silicon probe with a spring constant of ≈40 N/m under ambient conditions (24 °C, ≈45% RH). The resonance frequency of the cantilever is approximately 300 kHz. The surface roughness (S_q) of AFM images were calculated within a scanning area of 50 μm × 50 μm from three nearby (70 μm apart from the first images) locations.

3. Results and Discussion

3.1. Chemical Changes

Our prior study [34] investigated the chemical degradation of PET when exposed to different environmental factors, including 100% UV radiation, three temperatures (30 °C, 40 °C, and 50 °C), and two humidity levels (dry and saturated humidity). UV radiation can initiate photochemical reactions in PET, causing chain scission in PET to occur in the vinyl–ester bond at 1713 cm^{-1} and form new functional groups including carboxylic acid, which is confirmed by its presence at 1685 cm^{-1}. The chemical changes are evident on the surface exposed to UV radiation but are not observed on the unexposed or inner surface, as shown in Figure 2. As evidenced by the decrease in the intensity of the ester bond peak at 1713 cm^{-1} and the concurrent increase in the carboxylic acid peak at 1685 cm^{-1} in the FTIR spectra, the hydrolysis reaction is markedly more prevalent in SH environments (Figure 2a). Therefore, humidity and UV radiation have a synergistic effect on PET degradation. UV radiation can cause chain scission, and humidity can promote hydrolysis. The ester bond was found to decrease more rapidly in humid conditions with UV radiation than in dry conditions, suggesting that humidity is crucial for chain scission. In addition, temperature is a key factor affecting the chemical changes in PET, including the breakdown of the ester bond and the formation of carboxylic acid. The carbonyl index is slightly lower at 50 °C than at 30 °C under both dry and SH conditions (Figure 2b). Note that the carbonyl index is the indicator for quantifying the extent of PET degradation over time, and it was calculated by measuring the absorbance at the peak of 1713 cm^{-1} divided by the absorbance at the peak of 1685 cm^{-1} (ester/acid ratio) for the analysis of hydrolysis characterization. This means that PET undergoes thermal treatment and leads to the initiation breakdown of vinyl esters and the formation of a specific chemical compound, carboxylic acid, at a peak of 1685 cm^{-1}, which is higher at 50 °C compared to a lower temperature of 30 °C. The experimental results consistently demonstrated that PET undergoes significantly faster degradation when exposed to SH conditions (≥95% RH) compared to dry conditions (≤5% RH). This accelerated degradation can be attributed to the enhanced hydrolysis process, which involves the breakdown of the ester linkages within the PET polymer chains.

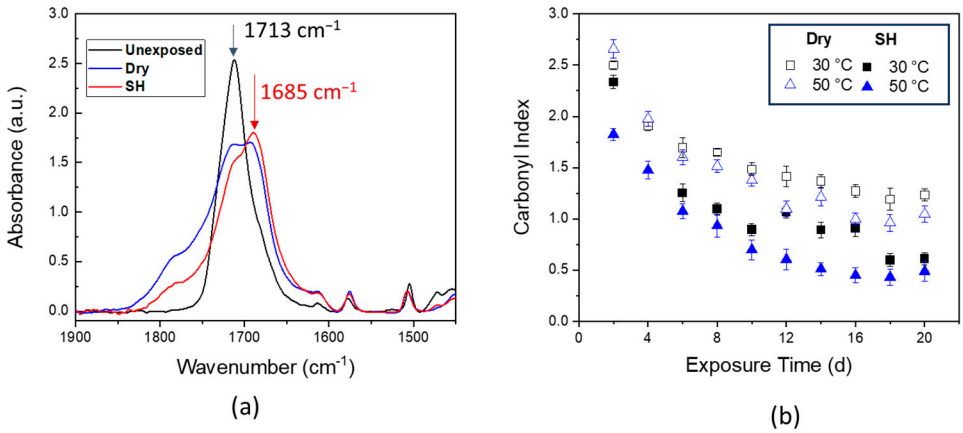

Figure 2. (**a**) FTIR spectra for PET under different exposure conditions. (**b**) Carbonyl index as a function of exposure time at different temperatures and humidities, as indicated in the legend. Measurement uncertainties were calculated using standard deviations (SDs) from 33 data points (n = 33). SDs were approximately 6%. Symbols represent the mean, and error bars indicate standard deviation (n = 33).

3.2. Surface Appearance and Morphological Changes

Figure 3 displays the photos of PET films after being exposed to SH (>95% RH) and dry conditions (≤5% RH) at two different temperatures after 20 days of exposure. PET films became cloudy and brittle (Figure 3a), and the opaqueness increased with increasing temperature (e.g., Figure 3c) and exposure time. In contrast, PET films under dry conditions (i.e., ≤5% RH) remained transparent and smooth (Figure 3b) and became slightly more yellow (Figure 3d) with increasing temperature and exposure time.

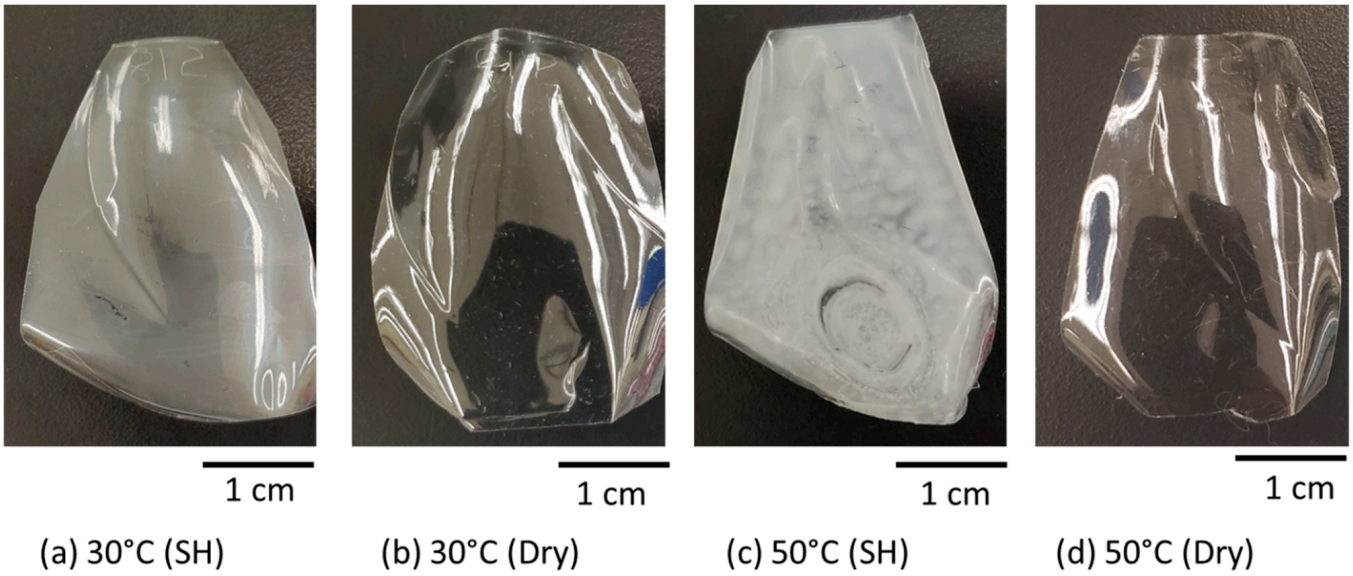

Figure 3. Photos of PET specimens after 20 days' exposure to UV/30 °C in (**a**) SH, (**b**) dry and UV/50 °C, (**c**) SH, and (**d**) dry conditions. Scale bar is 1 cm.

To investigate the appearance difference on the weathered surfaces, LSCM and AFM were carried out to characterize the surface morphology. Figure 4 displays PET specimens' surface morphology (LSCM images) after 20 days' exposure to UV/50 °C in SH and dry conditions. The weathered PET surfaces exhibited a significant increase in particle formation under SH conditions (Figure 4a). In contrast, dry conditions resulted in a minimal presence of particles, with a few exhibiting noticeable pits or indentations (Figure 4b). Furthermore, despite the notable transformation of the PET surfaces on the exposed side, the unexposed side (Figure 4c) remained smooth and free of particles. This result confirmed that water (moisture) plays a significant role in the formation of microplastic particles in plastic materials. To determine the chemical composition of the particles generated on the degraded surface (Figure 5a), the surface was scraped under both dry (not shown here) and SH (Figure 5b) conditions. These surface particles were associated with degradation products, for example, carboxylic acid. This was confirmed by the disappearance of the 1685 cm^{-1} peak after scraping the surface (Figure 5c). UV radiation primarily degrades PET through photo-oxidation, where the surface is most susceptible due to direct exposure. The degradation process, facilitated by the increased concentration of carboxylic acid, is a contributing factor to the formation of surface defects. Indeed, water trapped within the polymer acts as a plasticizer, reducing its mechanical strength and facilitating chemical degradation through hydrolysis reactions [44]. The findings indicate a correlation between the formation of carboxylic acid groups on the PET surface and the formation of microplastic particles in SH environments.

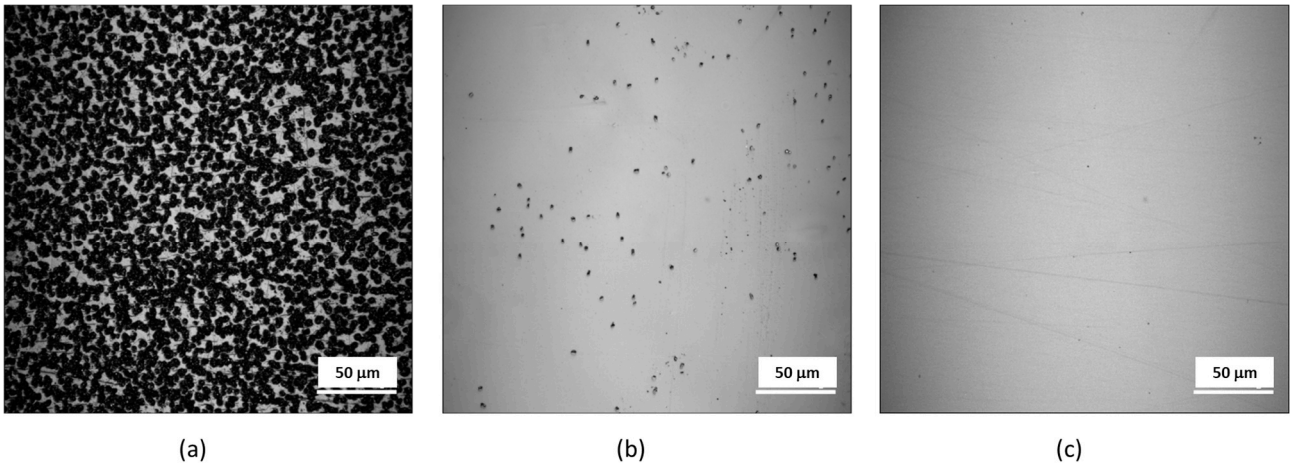

Figure 4. Surface morphology (LSCM images) of PET specimens after 20 days' exposure to UV/50 °C in (**a**) SH and (**b**) dry conditions. The unexposed surface is presented in (**c**) for comparison. The scale bar is 50 µm.

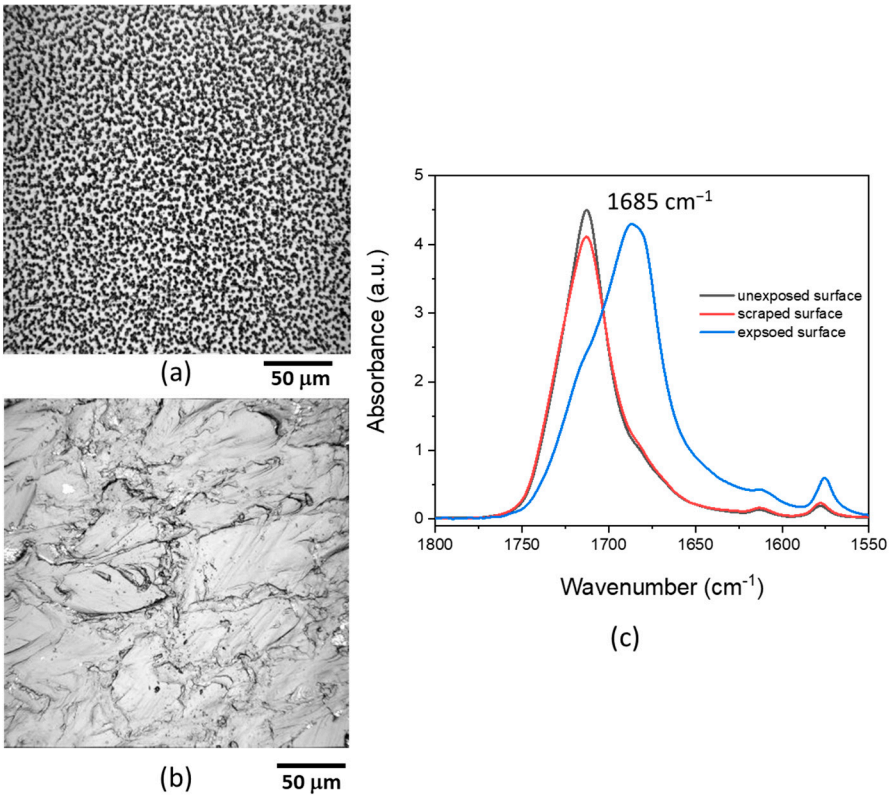

Figure 5. The surface morphology (**a**) at 20 days under 40 °C/SH conditions, (**b**) after scraping, and (**c**) the corresponding FTIR spectra. The scale bar is 50 µm.

To examine the topographic characteristics of microplastic particles closely, AFM measurements were conducted. Figure 6 displays the topography images of two samples subjected to different weathering conditions (SH and dry). Figure 6a,b illustrates samples exposed under SH conditions at different locations: (a) near the border (3 cm from the center of the sample holder) area and (b) in the center area of the exposure PIE cell. Note that the UV irradiance was higher in the center area ($\approx$ 276 MJ/m^2) than that near the border ($\approx$ 259 MJ/m^2). Figure 6a shows particles were not in the same plane. The height of the particles near the border ranges from 2 µm to 4 µm and particle size from 1 µm to 4 µm, exhibiting relatively high roughness with S_q = (830 $\pm$ 10) nm. In contrast, the particles

at the center area, with an average height of approximately 2.7 µm, display a relatively flat profile with S_q = (499 ± 8) nm. From Figure 6a–b, it appeared that particles began to grow with increasing UV dose and particles formed agglomerated continuous granules. However, unlike the topographic image, the phase image (not shown here) reveals low contrast in the samples. The phase contrast in these samples arises from the variation in hardness between the grown particles and the flat areas, while the particles that form on the surface are slightly softer than other areas. Figure 5c displays the sample exposed under dry conditions. The topography image of this sample shows fewer particle accumulations (S_q = 10.5 nm ± 1 nm) compared to that on the surface of the SH sample, and particles are much smaller with no phase differences. The AFM results indicate that the growth and formation of particle aggregation is sensitive to localized irradiance and moisture levels on the surface, and this reflects the heterogeneous distribution on the microscopic level.

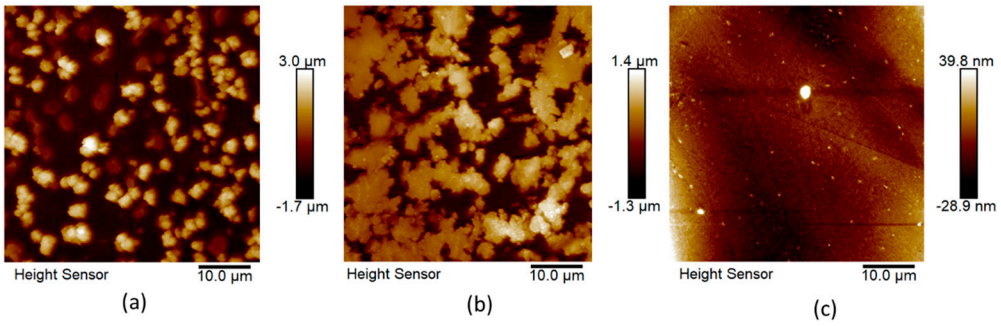

Figure 6. AFM height images of PET specimens after 20 days' exposure to UV/50 °C in SH at two different locations near (**a**) the border and (**b**) the center area of the PIE sample holder under SH and (**c**) dry conditions. Images are 50 µm × 50 µm.

This heterogeneous formation of particle aggregation on the weathered surface became more pronounced at a longer exposure time. As shown in Figure 6, for prolonged UV exposure in SH conditions (100% UV at 50 °C, 30 days of exposure) at two different locations, particles formed agglomerated continuous granules, and fragmentation occurred after further degradation. It is clearly displayed in the LSCM images (Figure 7) that surface morphologies (irregular cracks, fragmentation, surface roughness, etc.) are very different. Note that uneven yellowing was also observed visually throughout the samples. High temperatures can cause plastics to degrade thermally, breaking down their polymer chains. This can lead to reactions with oxygen, like photodegradation, resulting in the formation of radicals and other degradation products. Both chain scission and cross-linking are possible during thermal degradation [45]. Additionally, UV irradiation absorbed by polymer generates radicals, which then reacted with oxygen, forming chain scission products and oxidized chain ends. Radicals can also combine, leading to crosslinking. Extended exposure to humid conditions and elevated temperatures led to a progressive modification of the surface structure, leading to a loss of gloss, increased roughness, and the development of microcracks. Additionally, the plastics' chemical composition, physical structure, and shape are also expected to play a role in microplastic formation. These changes can accelerate the aging of the polymer, especially since the irregular cracks can grow into deeper layers of the particle, providing a site for fragmentation. This phenomenon could occur in the longer exposure time. A similar study also showed that a few microcracks were observed in the PET bottles immersed in seawater for 150 days, which may be caused by the combination of wind, waves, light, and other factors [30].

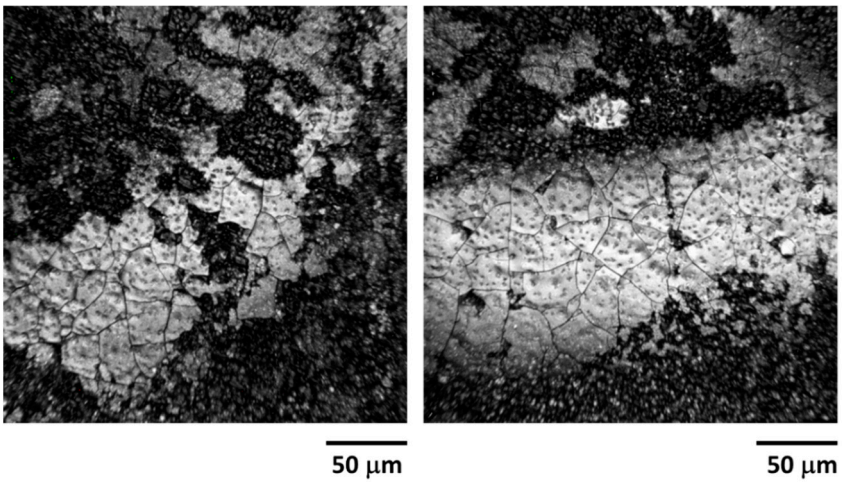

Figure 7. LSCM images (different locations) of PET surfaces exposed to 100% UV under 50 °C and SH conditions after 30 days of exposure. The scale bar is 50 µm.

3.3. Time Evolution of Microparticle Growth

The LSCM images in Figure 8 were selected from different exposure times and different temperatures to demonstrate the possible sequence of microplastic particle formation. As displayed in Figure 8, (a) small particles started to appear, (b) more particles appeared and particle size increased, (c) particles grew (in size/area as well as in height), (d) particles continued to grow and connect to adjacent particles, and (e) particles merged and formed agglomerated continuous granules, and some microcracks appeared on the surfaces. Note that some shallower microcracks were also observed in the earlier exposure time conditions; the cause of the microcracks is currently under investigation. Similar crack behavior was observed in Lin et al. [31] for photovoltaic backsheets under UV irradiations; however, the causes of the microcracks under environmental stress (UV, T, RH, mechanical) are very complex and highly dependent on the polymer type. To capture the accurate growth pattern and understand the mechanism of microplastic generation, an ongoing study to monitor the particles at the same locations is underway.

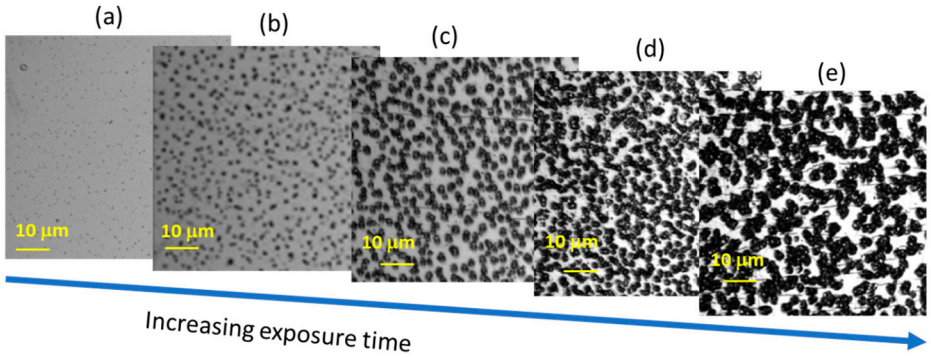

Figure 8. A series of LSCM images illustrates surface morphological changes and the growth of microplastic particles with increasing exposure time: (**a**) small particles appeared, (**b**,**c**) more particles appeared and particle size increased, (**d**,**e**) particles continued to grow, merge, and form agglomerates. The scale bar is 10 µm.

The dependence of surface morphological changes and the growth of microplastic particles on environmental conditions such as UV radiation, humidity, and temperature is shown in Figure 9. The particles generated at 50 °C are larger compared to those produced at 40 °C and 30 °C at the same exposure time in the SH conditions (Figure 9). Higher temperatures promoted carboxylic acid formation, particularly in the amorphous regions

where particles initially nucleate. A study found that high temperatures can accelerate the degradation of PET fibers, leading to brittleness and the formation of small cracks [29]. Additionally, elevated temperatures can induce thermal degradation and oxidation, resulting in the formation of new chemical groups such as vinyl ester and carboxyl end groups [29,34]. Another study indicated that UV-treated PET films buried in soil degraded, forming holes and microcracks. The material became brittle and fragmented into tiny particles [46]. As previously discussed, the hydrolysis process on PET surfaces resulted in the generation of particles, the size and quantity of which were significantly influenced by temperature. With increasing temperatures, the particles produced became larger in size. Additionally, the overall number of particles decreased due to the merging of smaller particles at higher temperatures, as visually depicted in Figure 9. The combined effects of humidity and temperature play a significant role in the formation and growth of particles on the PET surface. While the formation of particles was observed under both dry and SH conditions, the rate of particle growth and the final size of the particles were significantly different. In dry conditions, the formation of particles was less pronounced, and the size of the particles remained relatively constant over time. However, in SH conditions, the particles not only formed more rapidly, but also grew (in size) at a noticeable rate.

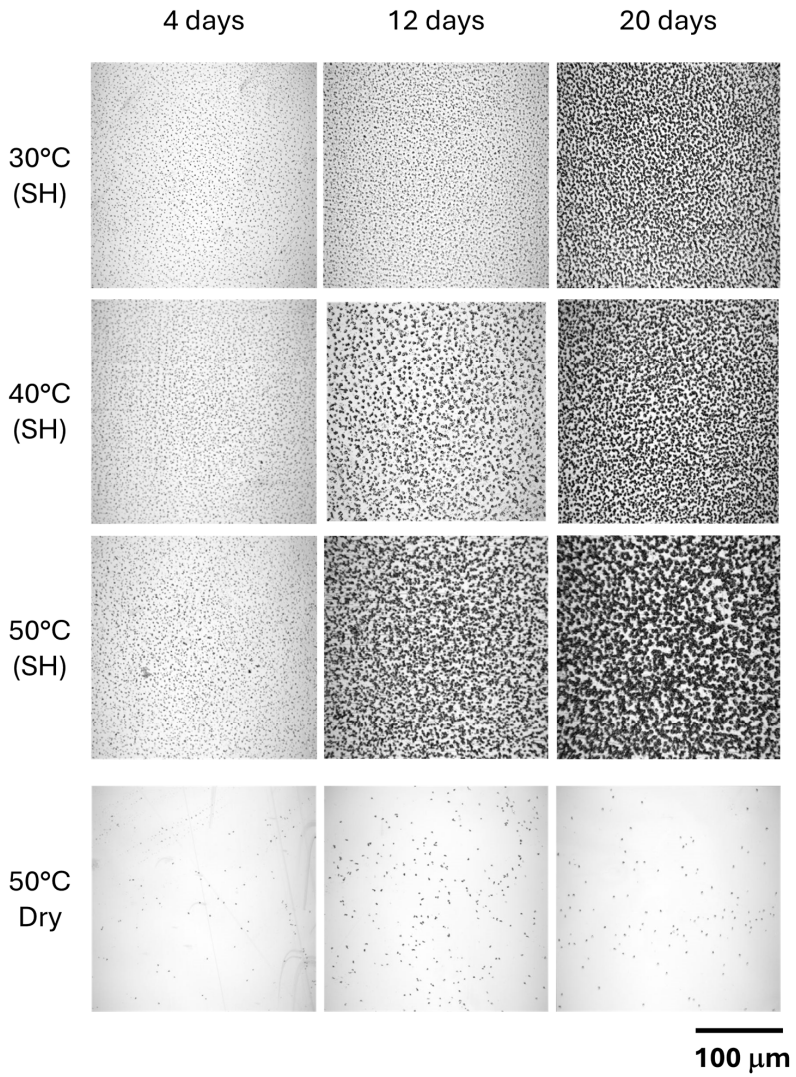

Figure 9. LSCM images of surface morphologies at different exposure times for three temperatures (30 °C, 40 °C, 50 °C) under SH conditions; the morphologies under 50 °C/dry conditions are also shown in the bottom row. The scale bar is 100 µm.

Figure 10a illustrates the relationship between apparent particle diameter and temperature for exposure times up to 12 days. Here, the apparent particle diameter was calculated by 2 × SQRT (occupied connected pixel area/π), assuming a sphere-like particle. As the particles continued to grow, merge, and form agglomerates (Figure 8d,e), the shape of agglomerates was far from a sphere. Therefore, this image analysis method for characterizing the quantity and size of the particles is only valid for sphere-like particles at earlier exposure times (<12 days). Additionally, due to the heterogeneous formation of particle aggregation at longer exposure times, the variance in particle size data becomes quite large at higher temperatures (50 °C). At 50 °C, particles are larger than at 30 °C and 40 °C, especially after 6 days of exposure. The particle diameter was around (1.70 ± 1.1) µm at 50 °C, (1.17 ± 0.53) µm at 40 °C, and (0.97 ± 0.44) µm 40 °C for 8 days of exposure time. This suggests that temperature strongly influences particle size over time. While the particle counts (Figure 10b) at 30 °C are initially higher due to the smaller size of particles, larger particles at 40 °C and 50 °C tend to agglomerate more readily, leading the software to recognize them as large individual particles, which results in a lower count after 8 days at 40 °C and 6 days at 50 °C, respectively.

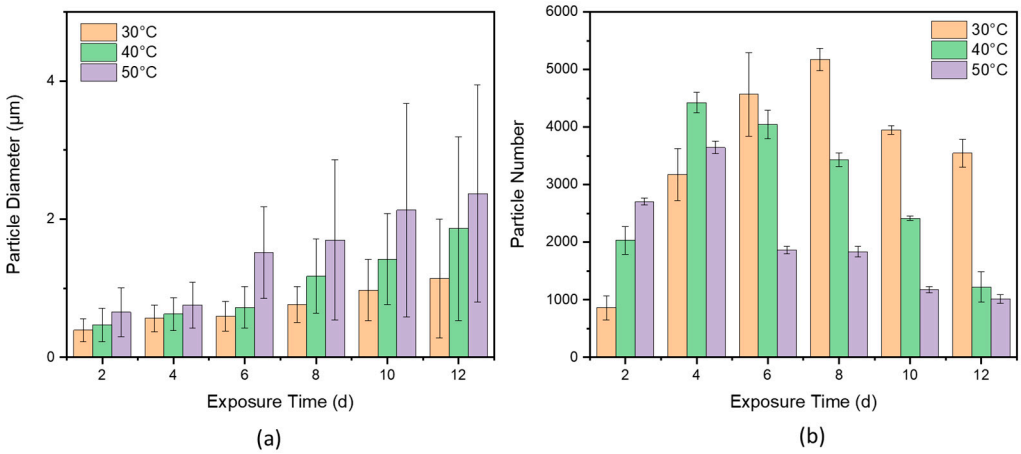

Figure 10. The (**a**) apparent diameter and (**b**) estimated particle count of surface particles at different exposure times for three temperatures (30 °C, 40 °C, 50 °C) under SH conditions. Measurement uncertainties were calculated using standard deviations (SDs) from at least 15 images (n = 15).

In addition to the formation of particles, another significant change observed during the degradation of PET in SH conditions is a marked increase in surface roughness. As depicted in Figure 11, the root-mean-square surface roughness (S_q) values remain relatively unchanged in dry conditions across different temperatures. However, in SH conditions, roughness increases with increasing exposure time; however, the differences in root-mean-square roughness (S_q) values were not statistically significant due to temperature variations. This observation is similar to the weak temperature dependence on the chemical degradation rate in terms of carbonyl index (small differences between 30 °C and 50 °C, as shown in Figure 2). The main reason can be attributed to the high glass transition temperature of the PET film. The glass transition temperature of PET is around 80 °C, and the PET remains in a similar glassy state between 30 °C and 50 °C. Other research found that LDPE films initially exhibited a smooth, homogeneous, and compact texture. However, upon UV irradiation, the surface developed roughness in the form of flakes, granular texture, and solution pits due to oxidation [47]. Additionally, another study mentioned that the degradation process led to morphological alterations at the macro/microscopic level, including discoloration, crazing, surface roughness, (micro)cracking, debris formation, changes in crystallinity, and cross-linking [42], which are consistent with the findings of this study. Another study

focused on Poly (ε-caprolactone) or PCL and found that, at 30% RH, completely smooth fibers were produced. Both 50% and 70% RH resulted in slight surface wrinkling, while 90% RH led to moderate surface roughness [48].

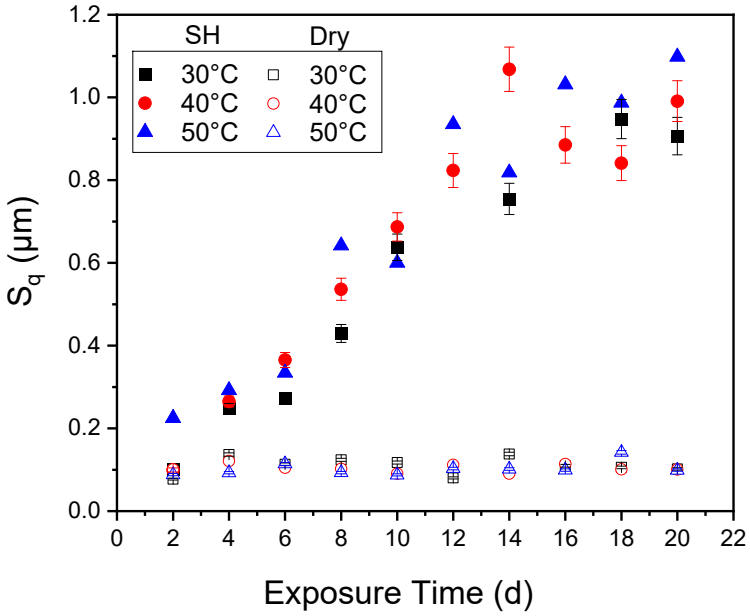

Figure 11. Surface roughness (S_q) at different exposure times for three temperatures (30 °C, 40 °C, 50 °C) under dry and SH conditions. Measurement uncertainties were calculated using standard deviations (SDs) from at least 15 images (n = 15). Symbols represent the mean, and error bars indicate standard deviation (n = 15).

4. Summary

This study investigated the interdependent effects of UV radiation, humidity, and temperature on the degradation of PET, a widely used plastic material. The findings of this study reveal that these environmental factors collectively contribute to the formation of cracks and particles on the PET surface. UV irradiation absorbed by polymers generates radicals which then react with oxygen, forming chain scission products and oxidized chain ends. Radicals can also combine, leading to cross-linking. High humidity levels (>95% RH) create a more conducive environment for degradation by increasing the moisture content of the PET material, promoting chemical reactions, and leading to the growth of microplastic particles and increasing surface roughness. Temperature significantly influences particle size and aggregation behavior. Higher temperatures accelerate the degradation process, leading to larger particles and a reduced particle count due to particle agglomeration. The roughness of PET films was observed to increase in saturated humidity conditions compared to dry conditions (<5% RH); however, the rate of changes in root-mean-square roughness (S_q) values were not statistically significant for temperatures ranging from 30 °C to 50 °C due to the high glass transition temperature (80 °C) of PET film. The in-depth investigation of crack formation and particle growth is underway.

Additionally, the formation of cracks in PET under UV exposure is a complex process influenced by photodegradation, hydrolysis, thermal degradation, and stress concentration. These factors can interact in various ways to influence the rate and extent of degradation. The further study of PET exposed to UV/temperature while immersed in the water/seawater is ongoing. It is important to note that the findings of this study are specific to the PET water bottles used and may not apply to other types of PET or other materials.

Author Contributions: Conceptualization, S.R., C.F., Y.L. and L.-P.S.; methodology, S.R., S.S.J., J.-K.H. and L.-P.S.; software, S.R., J.-K.H., R.C. and S.S.J.; validation, S.R., S.S.J., J.-K.H. and L.-P.S.; formal analysis, S.R., J.-K.H., R.C. and S.S.J.; investigation, S.R., J.-K.H. and S.S.J.; data curation, S.R., J.-K.H. and L.-P.S.; writing—original draft, S.R., J.-K.H. and C.F.; writing—review and editing, S.R., R.C., Y.L., C.F. and L.-P.S.; supervision, Y.L., C.F. and L.-P.S.; project administration, C.F. and L.-P.S.; funding acquisition, C.F., Y.L. and L.-P.S. All authors have read and agreed to the published version of the manuscript.

Funding: This study was supported by the NIST Circular Economy Program and the NIST PREP program with the Johns Hopkins University—Morgan State University HBCU Consortium. Additionally, Chunlei Fan received funding from Department of Energy (DOE) Biological and Environmental Research (BER) program under Contract DE-FOA-0002581, and partial funding from the National Science Foundation (award number 2022887). Chunlei Fan and Yuejin Li received partial funding from the National Institute on Minority Health and Health Disparities of the National Institutes of Health (award number U54MD013376). The content is solely the authors' responsibility and does not necessarily represent the official views of the National Institutes of Health.

Data Availability Statement: The raw/processed data required to reproduce these findings can be shared upon request and contingent upon the internal approval of the National Institute of Standards and Technology.

Acknowledgments: The author (S.R.) is deeply grateful to the Infrastructure Materials Group at NIST for the invaluable opportunity to access their facilities. The support provided by the NIST Circular Economy Program and the NIST PREP Program was instrumental to this work. Special thanks are extended to Deborah Jacobs and Karissa Jensen for their dedicated maintenance of the NIST SPHERE during the weathering experiments.

Conflicts of Interest: The authors assert that they have no known competing financial interests or personal relationships that could be perceived as influencing the work reported in this paper.

NIST Disclaimer: Specific commercial products or equipment are described in this paper to adequately specify the experimental procedure. In no case does such identification imply recommendation or endorsement by the National Institute of Standards and Technology, nor does it mean that using the best available for the purpose is necessary.

References

1. Ma, H.; Pu, S.; Liu, S.; Bai, Y.; Mandal, S.; Xing, B. Microplastics in aquatic environments: Toxicity to trigger ecological consequences. *Environ. Pollut.* **2020**, *261*, 114089. [CrossRef] [PubMed]
2. Wang, Y.; Zhang, Y.; Song, H.; Wang, Y.; Deng, T.; Hou, X. Zinc-catalyzed ester bond cleavage: Chemical degradation of polyethylene terephthalate. *J. Clean. Prod.* **2019**, *208*, 1469–1475. [CrossRef]
3. Gardette, J.L.; Colin, A.; Trivis, S.; German, S.; Therias, S. Impact of photooxidative degradation on the oxygen permeability of poly(ethyleneterephthalate). *Polym. Degrad. Stab.* **2014**, *103*, 35–41. [CrossRef]
4. Ghanbari, A.; Heuzey, M.C.; Carreau, P.J.; Ton-That, M.T. A novel approach to control thermal degradation of PET/organoclay nanocomposites and improve clay exfoliation. *Polymer* **2013**, *54*, 1361–1369. [CrossRef]
5. Zekriardehani, S.; Jabarin, S.A.; Gidley, D.R.; Coleman, M.R. Effect of Chain Dynamics, Crystallinity, and Free Volume on the Barrier Properties of Poly(ethylene terephthalate) Biaxially Oriented Films. *Macromolecules* **2017**, *50*, 2845–2855. [CrossRef]
6. Sang, T.; Wallis, C.J.; Hill, G.; Britovsek, G.J.P. Polyethylene terephthalate degradation under natural and accelerated weathering conditions. *Eur. Polym. J.* **2020**, *136*, 109873. [CrossRef]
7. Falkenstein, P.; Gräsing, D.; Bielytskyi, P.; Zimmermann, W.; Matysik, J.; Wei, R.; Song, C. UV Pretreatment Impairs the Enzymatic Degradation of Polyethylene Terephthalate. *Front. Microbiol.* **2020**, *11*, 689. [CrossRef]
8. Manzoor, S.; Naqash, N.; Rashid, G.; Singh, R. Plastic Material Degradation and Formation of Microplastic in the Environment: A Review. *Mater. Today Proc.* **2022**, *56*, 3254–3260. [CrossRef]
9. Koshti, R.; Mehta, L.; Samarth, N. Biological Recycling of Polyethylene Terephthalate: A Mini-Review. *J. Polym. Environ.* **2018**, *26*, 3520–3529. [CrossRef]
10. van Wezel, A.; Caris, I.; Kools, S.A.E. Release of primary microplastics from consumer products to wastewater in the Netherlands. *Environ. Toxicol. Chem.* **2016**, *35*, 1627–1631. [CrossRef]

11. Petersen, E.J.; Barrios, A.C.; Henry, T.B.; Johnson, M.E.; Koelmans, A.A.; Montoro Bustos, A.R.; Matheson, J.; Roesslein, M.; Zhao, J.; Xing, B. Potential Artifacts and Control Experiments in Toxicity Tests of Nanoplastic and Microplastic Particles. *Environ. Sci. Technol.* **2022**, *56*, 15192–15206. [CrossRef] [PubMed]
12. Ding, L.; Yu, X.; Guo, X.; Zhang, Y.; Ouyang, Z.; Liu, P.; Zhang, C.; Wang, T.; Jia, H.; Zhu, L. The photodegradation processes and mechanisms of polyvinyl chloride and polyethylene terephthalate microplastic in aquatic environments: Important role of clay minerals. *Water Res.* **2022**, *208*, 117879. [CrossRef] [PubMed]
13. Chia, R.W.; Lee, J.Y.; Kim, H.; Jang, J. Microplastic pollution in soil and groundwater: A review. *Environ. Chem. Lett.* **2021**, *19*, 4211–4224. [CrossRef]
14. Torres, F.G.; Dioses-Salinas, D.C.; Pizarro-Ortega, C.I.; De-la-Torre, G.E. Sorption of chemical contaminants on degradable and non-degradable microplastics: Recent progress and research trends. *Sci. Total Environ.* **2021**, *757*, 143875. [CrossRef]
15. Qin, M.; Chen, C.; Song, B.; Shen, M.; Cao, W.; Yang, H.; Zeng, G.; Gong, J. A review of biodegradable plastics to biodegradable microplastics: Another ecological threat to soil environments? *J. Clean. Prod.* **2021**, *312*, 127816. [CrossRef]
16. Jakubowska, M.; Białowąs, M.; Stankevičiūtė, M.; Chomiczewska, A.; Jonko-Sobuś, K.; Pažusienė, J.; Hallmann, A.; Bučaitė, A.; Urban-Malinga, B. Effects of different types of primary microplastics on early life stages of rainbow trout (*Oncorhynchus mykiss*). *Sci. Total Environ.* **2022**, *808*, 151909. [CrossRef]
17. Guan, M.; Jin, H.; Wei, W.; Yan, M. Degradation of polyethylene terephthalate (PET) and polypropylene (PP) plastics in seawater. *DeCarbon* **2023**, *1*, 100006. [CrossRef]
18. Belioka, M.-P.; Achilias, D.S. The Effect of Weathering Conditions in Combination with Natural Phenomena/Disasters on Microplastics' Transport from Aquatic Environments to Agricultural Soils. *Microplastics* **2024**, *3*, 518–538. [CrossRef]
19. Smith, M.; Love, D.C.; Rochman, C.M.; Neff, R.A. Microplastics in Seafood and the Implications for Human Health. *Curr. Environ. Health Rep.* **2018**, *5*, 375–386. [CrossRef]
20. De-la-Torre, G.E. Microplastics: An emerging threat to food security and human health. *J. Food Sci. Technol.* **2020**, *57*, 1601–1608. [CrossRef]
21. Winiarska, E.; Jutel, M.; Zemelka-Wiacek, M. The potential impact of nano- and microplastics on human health: Understanding human health risks. *Environ. Res.* **2024**, *251*, 118535. [CrossRef] [PubMed]
22. Campanale, C.; Massarelli, C.; Savino, I.; Locaputo, V.; Uricchio, V.F. A detailed review study on potential effects of microplastics and additives of concern on human health. *Int. J. Environ. Res. Public Health* **2020**, *17*, 1212. [CrossRef] [PubMed]
23. Prata, J.C.; da Costa, J.P.; Lopes, I.; Duarte, A.C.; Rocha-Santos, T. Environmental exposure to microplastics: An overview on possible human health effects. *Sci. Total Environ.* **2020**, *702*, 134455. [CrossRef] [PubMed]
24. Emenike, E.C.; Okorie, C.J.; Ojeyemi, T.; Egbemhenghe, A.; Iwuozor, K.O.; Saliu, O.D.; Okoro, H.K.; Adeniyi, A.G. From oceans to dinner plates: The impact of microplastics on human health. *Heliyon* **2023**, *9*, e20440. [CrossRef]
25. Dong, M.; Zhang, Q.; Xing, X.; Chen, W.; She, Z.; Luo, Z. Raman spectra and surface changes of microplastics weathered under natural environments. *Sci. Total Environ.* **2020**, *739*, 139990. [CrossRef]
26. Andrady, A.L.; Law, K.L.; Donohue, J.; Koongolla, B. Accelerated degradation of low-density polyethylene in air and in sea water. *Sci. Total Environ.* **2022**, *811*, 151368. [CrossRef]
27. Menzel, T.; Meides, N.; Mauel, A.; Mansfeld, U.; Kretschmer, W.; Kuhn, M.; Herzig, E.M.; Altstädt, V.; Strohriegl, P.; Senker, J.; et al. Degradation of low-density polyethylene to nanoplastic particles by accelerated weathering. *Sci. Total Environ.* **2022**, *826*, 154035. [CrossRef]
28. Fabiyi, J.S.; McDonald, A.G. Physical morphology and quantitative characterization of chemical changes of weathered PVC/pine composites. *J. Polym. Environ.* **2010**, *18*, 57–64. [CrossRef]
29. Asadi, H.; Uhlemann, J.; Stranghoener, N.; Ulbricht, M. Artificial weathering mechanisms of uncoated structural polyethylene terephthalate fabrics with focus on tensile strength degradation. *Materials* **2021**, *14*, 618. [CrossRef]
30. Wu, B.; Wu, H.; Xu, S.M.; Wang, Y.Z. Comparative study of the aging degradation behaviors of PET under artificially accelerated and typical marine environment. *Polym. Degrad. Stab.* **2023**, *217*, 110515. [CrossRef]
31. Lin, C.C.; Lyu, Y.; Jacobs, D.S.; Kim, J.H.; Wan, K.T.; Hunston, D.L.; Gu, X. A novel test method for quantifying cracking propensity of photovoltaic backsheets after ultraviolet exposure. *Prog. Photovolt. Res. Appl.* **2019**, *27*, 44–54. [CrossRef]
32. Pinlova, B.; Nowack, B. From cracks to secondary microplastics—Surface characterization of polyethylene terephthalate (PET) during weathering. *Chemosphere* **2024**, *352*, 141305. [CrossRef] [PubMed]
33. Thushari, G.G.N.; Senevirathna, J.D.M. Plastic pollution in the marine environment. *Heliyon* **2020**, *6*, e04709. [CrossRef] [PubMed]
34. Rostampour, S.S.; Cook, R.; Jhang, S.-S.; Li, Y.; Fan, C.; Sung, L.-P. Changes in the Chemical Composition of PolyethyleneTerephthalate under UV Radiation in Various Environmental Conditions. *Polymers* **2024**, *16*, 2249. [CrossRef]
35. Gok, A.; Ngendahimana, D.K.; Fagerholm, C.L.; French, R.H.; Sun, J.; Bruckman, L.S. Predictive models of poly(ethyleneterephthalate) film degradation under multifactor accelerated weathering exposures. *PLoS ONE* **2017**, *12*, 0177614. [CrossRef]

36. Gordon, D.A.; Huang, W.H.; Burns, D.M.; French, R.H.; Bruckman, L.S. Multivariate multiple regression models of poly(ethylene-terephthalate) film degradation under outdoor and multi-stressor accelerated weathering exposures. *PLoS ONE* **2018**, *13*, 0209016. [CrossRef]
37. Dimassi, S.N.; Hahladakis, J.N.; Yahia, M.N.D.; Ahmad, M.I.; Sayadi, S.; Al-Ghouti, M.A. Insights into the degradation mechanism of PET and PP under marine conditions using FTIR. *J. Hazard. Mater.* **2023**, *447*, 130796. [CrossRef]
38. Fotopoulou, K.N.; Karapanagioti, H.K. Degradation of Various Plastics in the Environment. *Handb. Environ. Chem.* **2019**, *78*, 71–92. [CrossRef]
39. Miranda, M.N.; Sampaio, M.J.; Tavares, P.B.; Silva, A.M.T.; Pereira, M.F.R. Aging assessment of microplastics (LDPE, PET and uPVC) under urban environment stressors. *Sci. Total Environ.* **2021**, *796*, 148914. [CrossRef]
40. Pickett, J.E.; Kuvshinnikova, O.; Sung, L.P.; Ermi, B.D. Accelerated weathering parameters for some aromatic engineering thermoplastics. *Polym. Degrad. Stab.* **2019**, *166*, 135–144. [CrossRef]
41. Pickett, J.E.; Gardner, M.M.; Gilbson, D.A.; Rice, S.T. Goal Weathering of Aromatic Engineering Thermoplastics. *Polym. Degrad. Stab.* **2005**, *90*, 405–415. [CrossRef]
42. Lankone, R.; Zammarano, M.; Jhang, S.S.; Kaim, I.; Goodwin, D.G.; Kuo, Y.-T.; Sarti, G.; Gardi, S.; Cardeli, C.; Sung, L.P. *Effects of Weathering and Formulation on the Properties of Vinyl Siding*; NIST Technical Note (TN) NIST TN 2304; National Institute of Standards and Technology: Gaithersburg, MD, USA, 2024. [CrossRef]
43. *ISO 25178-2:2021*; Geometrical Product Specifications (GPS)—Surface Texture: Areal—Part 2: Terms, Definitions and Surface Texture Parameters). ISO: Geneva, Switzerland, 2021.
44. Nisticò, R. Polyethylene terephthalate (PET) in the packaging industry. *Polym. Test.* **2020**, *90*, 106707. [CrossRef]
45. Zhang, K.; Hamidian, A.H.; Tubić, A.; Zhang, Y.; Fang, J.K.; Wu, C.; Lam, P.K. Understanding plastic degradation and microplastic formation in the environment: A review. *Environ. Pollut.* **2021**, *274*, 116554. [CrossRef]
46. Iñiguez, M.E.; Conesa, J.A.; Fullana, A. Recyclability of four types of plastics exposed to UV irradiation in a marine environment. *Waste Manag.* **2018**, *79*, 339–345. [CrossRef] [PubMed]
47. Ranjan, V.P.; Goel, S. Degradation of Low-Density Polyethylene Film Exposed to UV Radiation in Four Environments. *J. Hazard. Toxic Radioact. Waste* **2019**, *23*, 04019015. [CrossRef]
48. Szewczyk, P.K.; Stachewicz, U. The impact of relative humidity on electrospun polymer fibers: From structural changes to fiber morphology. *Adv. Colloid Interface Sci.* **2020**, *286*, 102315. [CrossRef]